Photosynth Res (2009) 102:305–310
DOI 10.1007/s11120-009-9442-2

REVIEW

Introduction to magnetic resonance methods in photosynthesis

Martina Huber

Received: 27 February 2009 / Accepted: 19 May 2009 / Published online: 1 July 2009

Abstract Electron paramagnetic resonance (EPR) and, more recently, solid-state nuclear magnetic resonance (NMR) have been employed to study photosynthetic processes, primarily related to the light-induced charge separation. Information obtained on the electronic structure, the relative orientation of the cofactors, and the changes in structure during these reactions should help to understand the efficiency of light-induced charge separation. A short introduction to the observables derived from magnetic resonance experiments is given. The relation of these observables to the electronic structure is sketched using the nitroxide group of spin labels as a simple example.

Keywords Magnetic resonance · EPR · NMR · Photosynthesis · Nitroxides

Introduction

Photosynthesis has once been declared a heaven for magnetic resonance spectroscopy (Feher 1998). Initially, EPR was in the foreground, profiting from the wealth of species possessing unpaired electrons. More recently, NMR spectroscopy has also gained ground. While NMR, and certainly solution NMR, is an established subject in the curriculum of (bio)chemical studies, the exposure to EPR is more limited. Furthermore, in contrast to EPR, for NMR there is a wide choice of textbooks geared at audiences of different levels, from a compact text treating solution NMR (Hore 1995) to solid-state NMR introductory textbooks (Duer 2002; Levitt 2008). Given that the coverage for EPR is less complete in this respect, the focus of the present introduction is on EPR.

Magnetic resonance in general is treated in a few classical textbooks (Slichter 1996; Carrington and McLachlan 1979), and most of the introductory textbooks for EPR were written in the second half of the last century. Some of these have come out in more recent editions making them available to the public again (Weil and Bolton 2007; Atherton 1993). Modern pulsed EPR techniques are covered in a monograph bridging the gap between the traditionally used continuous-wave EPR methods and pulsed EPR (Schweiger and Jeschke 2001). The properties of the electron spin, such as T_2 relaxation times in the ns-range and spectral widths that can range from 30 MHz to thousands of MHz, make pulsed methods in EPR technically more demanding than in NMR. Therefore, pulsed methods are a much more recent development in EPR than in NMR.

The present introduction starts by identifying the parameters defining the resonance of an EPR or an NMR line. These parameters already contain information about the molecular and electronic structure of the center associated with the spin, e.g., the photosynthetic cofactor containing an unpaired electron or nuclei with a magnetic moment. Next are spin interactions, followed by a few examples which illustrate these points. Conceptually simple examples were chosen, since they allow the discussion of the phenomena without going into the detail that is at the heart of the research presented in the following sections.

M. Huber (✉)
Department of Molecular Physics, Leiden University,
P.O. Box 9504, 2300RA Leiden, The Netherlands
e-mail: mhuber@molphys.leidenuniv.nl

Fundamental magnetic resonance parameters

Electron and nuclear spin in the magnetic field

Electron and nuclear spins are aligned in an external magnetic field. For the electron with a spin quantum number $S = 1/2$ and for the nuclei with a nuclear quantum number $I = 1/2$, two energy levels result. The energy difference between the two levels is given by the resonance condition (Eq. 1).

$$\begin{aligned} \text{EPR} &: \Delta E = h\nu = g_e \beta_e B_0 \\ \text{NMR} &: \Delta E = h\nu = (1-\sigma) g_n \beta_n B_0 \end{aligned} \quad (1)$$

Here, ν is the frequency, B_0 is the static magnetic field at which the resonance occurs, g_e and g_n are the electron and nuclear g-factors, respectively, β_e and β_n are the Bohr and the nuclear magnetons, respectively, and σ is the chemical shielding.

Figure 1 shows the energy levels as a function of the magnetic field. Transitions between these energy levels can be induced by electromagnetic radiation resulting in an EPR or NMR resonance line. The resonance frequencies in EPR are in the microwave range, typically from 9 to several 100 GHz at magnetic fields from 0.3 to 12 T, and in NMR from several hundred to 900 MHz at magnetic fields from a few T to around 20 T. To define the resonance position of such a line, two parameters are needed: the magnetic field B_0 and the frequency of the electromagnetic radiation ν. In EPR, the position of the line is defined by g, the g-factor. In NMR, the chemical shielding σ plays that role. To define the resonance of nuclei independent of the measurement field, the chemical shift δ is introduced.

$$\delta = 10^6 \frac{(\nu - \nu_{ref})}{\nu_{ref}} = \frac{(\sigma_{ref} - \sigma)}{1 - \sigma_{ref}} \approx 10^6 (\sigma_{ref} - \sigma) \quad (2)$$

The chemical shift parameter δ is dimensionless and is given in ppm, parts per million (Hore 1995).

The g-value and the g-tensor

The g-value is one of the indicators of the type of paramagnetic center. A free electron has a g-value of $g_e = 2.002319$. Radicals or transition metal ions containing unpaired electrons have g-values that differ from g_e. The magnitude of the deviation is determined by the spin-orbit coupling parameters of the nuclei, which increase with the atomic mass. Two important radicals in the primary processes of photosynthesis, the chlorophyll-cation radicals and the quinone-anion radicals, serve as examples. For both types of radicals, the unpaired electron is delocalized over a π-electron system. In the chlorophyll-cation radical, the unpaired electron interacts mainly with carbon and proton nuclei. In EPR, even the carbon nucleus can be considered 'light' and its spin-orbit coupling parameter is not large enough to cause a significant deviation from the free electron g-value. Therefore, for chlorophyll-cation radicals the deviation from g_e is small and typically the g-value is found to be 2.0025 (Savitzky and Möbius 2009). Quinone-anion radicals have significantly more spin density at oxygen than the chlorophyll radicals, and their g-values are close to 2.0046 (Savitzky and Möbius 2009). While this difference gives rise to a separation in the field of several tenths of milli-Tesla (mT) in conventional 9 GHz EPR (X-band EPR), high-field EPR (35 GHz, Q-band and higher) is advantageous to discriminate the two types of radicals, and at 360 GHz, a separation of ca.12 mT results (Savitzky and Möbius 2009).

Larger spin-orbit coupling parameters also enhance the anisotropy of g, which makes the resonance dependent on the orientation of the molecule, or the metal-ligand system relative to the static magnetic field B_0. Such orientation dependence, anisotropy, is typical of the magnetic properties of electrons and nuclei and leads to the description of the property in question as a tensor, such as the g-tensor (**G**). The g-tensor is characterized by three principal values, g_{xx}, g_{yy}, and g_{zz}, each corresponding to a particular orientation of the molecule in the magnetic field B_0. In Fig. 2, this is illustrated for a simple radical, the nitroxide spin label. At the heart of these very stable radicals is the nitroxide group, in which the unpaired electron is delocalized over two centers, a nitrogen and an oxygen atom. A molecule that is aligned with the N–O bond, i.e., the

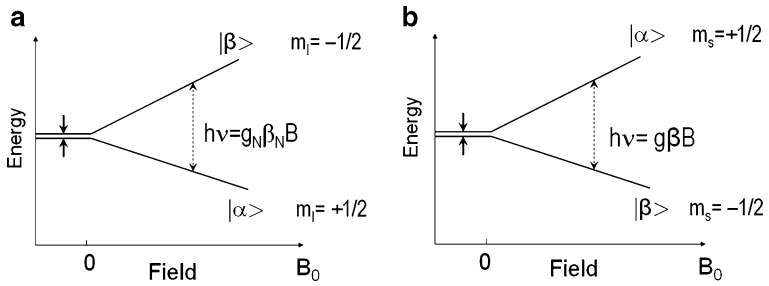

Fig. 1 Splitting of the energy levels of a nucleus ($I = 1/2$; left) and of an unpaired electron (spin $S = 1/2$; right) as a function of the external magnetic field B_0. In NMR, for typical fields of several T, the electromagnetic radiation is in the radiofrequency range (MHz); in EPR, for fields of up to several T, frequencies are in the microwave range (GHz)

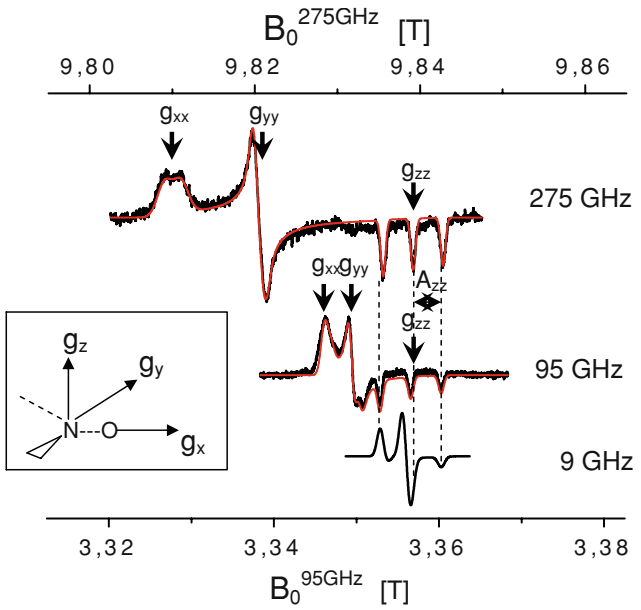

Fig. 2 EPR spectra taken at increasing magnetic field/frequency strengths showing the increased spectral resolution obtained by high-field/high-frequency EPR. Shown is the frozen solution spectrum of a nitroxide spin label at 9 GHz (X-band), 95 GHz (W-band, bottom scale), and 275 GHz (J-band, top scale). All spectra have the same relative B_0-field scale. The g-tensor components g_{xx}, g_{yy}, and g_{zz} become increasingly separated. The separation (A_{zz}) between the three lines at the high field side high field of the spectra remains constant, owing to the independence of the hyperfine splitting from the external magnetic field. Figure modified from Finiguerra et al. (2006)

g_x-direction parallel to the magnetic field, absorbs at the low field end of the spectrum, marked as g_{xx} in Fig. 2, a molecule for which B_0 is parallel to g_z at the high-field end of the spectrum. Therefore, molecules with specific orientations can be selected by their resonance position, making it possible to detect orientation effects in a random sample. The differences in g-values of two radicals, or the g-anisotropy of individual centers, become better resolved in high-field/high-frequency EPR. This is also illustrated in Fig. 2, where a spectrum obtained by conventional 9 GHz EPR is compared to spectra obtained at 95 GHz and at 275 GHz.

Orientation selection has been used to determine the relative orientations of the paramagnetic centers in photosynthesis (van der Est 2009; Savitzky and Möbius 2009; Kothe and Thurnauer 2009).

Chemical shifts

The chemical shift of nuclear resonances in NMR derives from the shielding of the external magnetic field at the position of the nucleus, which is caused by the magnetic field induced by the circulation of electrons in the molecule (Carrington and McLachlan 1979). So the electron density in the vicinity of the observed nucleus is important, and electron donating and withdrawing groups have a well-established effect on the chemical shift of the magnetic nuclei in a molecule. Chemical shift differences in the order of 10 ppm are common for protons, 200 ppm for ^{13}C nuclei. In a 400 MHz NMR spectrometer (9.4 T) the proton chemical shift range corresponds to a spread in the frequency of the lines of only 4 kHz. The magnetic field of an unpaired electron overwhelms this effect by far, since hyperfine splittings can be in the order of ten to hundreds of MHz, and therefore nuclei in the vicinity of or coupled to such an unpaired electron are shifted so far in the field that they cannot be observed under the usual conditions.

Dipolar spin–spin interactions

The interactions of electron and nuclear spins are often dipolar. Generally, a dipolar interaction between two magnetic moments μ_1 and μ_2 is given by

$$\Delta E = \frac{\vec{\mu_1}\vec{\mu_2}}{r^3} - \frac{(\vec{\mu_1}\vec{r})(\vec{\mu_2}\vec{r})}{r^5}. \quad (3)$$

Here **r** is the vector joining the two magnetic moments. Working out the scalar vector products under the condition that μ_1 and μ_2 are parallel results in

$$\Delta E = \frac{\mu_1\mu_2(1-\cos^2\theta)}{r^3}, \quad (4)$$

where θ is the angle between **r** and the magnetic field. For fast molecular tumbling the dipolar interaction averages to zero, leading to narrow lines and isotropic spectra. The sum over all possible angles θ, as observed on a random sample in the immobilized state, results in a powder pattern, the Pake pattern. In solid-state NMR the sample is rotated about an axis that has an angle θ of $\theta_{MA} = 53.4°$ with respect to the magnetic field. Since the magnitude of $\cos\theta_{MA}$ is zero, the dipolar interactions cancel out and therefore narrow lines are observed even in the solid state (Matysik et al. 2009; Alia et al. 2009).

Electron–electron interactions

The primary reactions of photosynthesis comprise single electron transfer reactions; therefore coupled radicals and radical pairs abound. The interactions between electron spins located on different cofactors have revealed a wealth of information on the distances and relative orientation of the radicals. Over short distances, exchange interactions need to be considered, but in the distance range between most of the cofactors, several nm, the dominant part of the interaction is dipolar. Several experiments have been designed in magnetic resonance to exploit electron–electron interactions in photosynthetic systems (van der Est 2009; Kothe and Thurnauer 2009; Matysik et al. 2009; Alia

et al. 2009). Ultimately, complete quantum mechanical understanding of the interactions within the radical pairs should reveal the mechanisms responsible for the high efficiency of photosynthetic electron transfer.

Electron–nuclear (hyperfine) interactions

The hyperfine interaction between an electron spin and a nuclear spin has two components: the isotropic, Fermi-contact interaction and a dipole–dipole term. The latter can be used to determine the location of protons and other nuclei in the vicinity of a center carrying spin density. One example for an application is the assignment of the protons hydrogen-bonded to the quinones in bacterial reaction centers (Flores et al. 2007). The Fermi-contact term derives from spin density in the s-orbital of the nucleus in question. For radicals with a delocalized π-electron system, the isotropic hyperfine interaction allows mapping the wavefunction at every position in the radical that has a suitable nucleus. Thereby, the wavefunction containing the unpaired electron is measured. The hyperfine interaction serves as a local probe of the MO coefficients, yielding a wealth of information on the electronic structure. To determine hyperfine couplings of the protons in π-radicals such as the bacteriochlorophyll radicals, EPR is not sufficient. Hyperfine couplings are in the range of several MHz, and EPR spectra are broadened by the interaction with several nuclei. Better resolution is obtained by electron–nuclear double resonance (ENDOR) (Kulik and Lubitz 2009) and pulsed EPR methods (van Gastel 2009).

In the bacterial reaction center, the cation or anion radicals of the cofactors have been investigated. One can stabilize the cation radical of the primary electron donor to obtain the spin density in the HOMO, the highest occupied molecular orbital, and the anion radicals of the electron acceptors, in which the unpaired electron is in the LUMO, lowest unoccupied molecular orbital. More recently, the triplet state of electron donors in photosynthesis became amenable to investigation (van Gastel 2009). In this state, the HOMO and the LUMO coefficients of the electron donor are obtained, revealing the distribution of the MO from which the electron leaves the cofactor (LUMO) and the MO which will accept the electron in the eventual charge recombination event. The relation between the light-induced reactions and the orbitals mentioned are discussed elsewhere in this issue (Carbonera 2009).

Electronic structure from EPR and NMR

Information from the hyperfine and the *G*-tensors

Advanced methods, such as solid-state NMR (Alia et al. 2009; Matysik et al. 2009), pulsed EPR (van Gastel 2009), and ENDOR (Kulik and Lubitz 2009), yield magnetic resonance parameters with high accuracy. To link these parameters to the electronic structure, quantum chemistry is used, and in many cases further method development in this area was driven by the desire to interpret magnetic resonance parameters. To describe the development in the interpretation of magnetic resonance parameters is beyond the scope of this account, but as above we will illustrate the essence using the nitroxide spin labels. Their π-electron system comprises only two atoms, the nitrogen and the oxygen atom, substantially simplifying the discussion compared to a molecule such as the chlorophyll, for example.

Hyperfine interaction

The spin-density distribution can be obtained from the hyperfine interaction of the unpaired electron with the nitrogen nuclear spin ($I = 1$). The interaction gives rise to the three lines separated by A_{zz} in Fig. 2. Overlap of the N and O p_z-orbitals results in the doubly occupied π-orbital and the singly occupied π^*-orbital (MO scheme, Fig. 3). The energy of the N versus the O p_z-orbital determines the magnitude of the MO coefficient on N, and thereby the hyperfine coupling of N. If the polarity in the vicinity of the NO group increases, the energy of the p_z-orbital on oxygen will decrease relative to the energy of the nitrogen p_z-orbital. As a result, the π^*-orbital will have a larger N character or, in other words, the MO coefficient on N will be larger, resulting in a larger nitrogen hyperfine coupling.

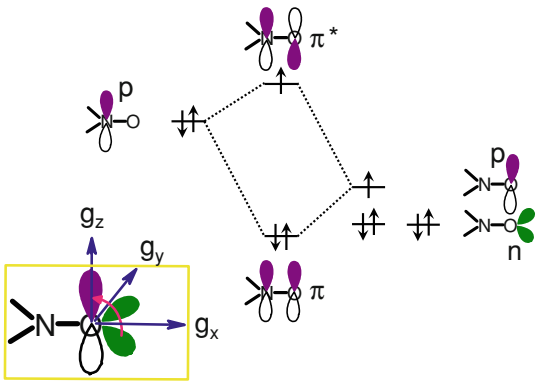

Fig. 3 Top: Schematic representation of the frontier orbitals of the nitroxide group. Left: p_z-type orbital on nitrogen; right: p_z- and non-bonding (*n*-) orbitals on oxygen. Polarity changes in the environment will shift the energy of the nitrogen p_z relative to the oxygen p_z-orbital, shifting spin density from nitrogen to oxygen. The spin density at nitrogen determines the electron-nitrogen hyperfine splitting, which therefore is a measure for polarity. Hydrogen bonding to the oxygen atom changes the energy of the *n*-orbitals relative to the π^*-orbital. This changes the energy required for n–p excitation and results in a shift in g_{xx} (bottom). Therefore, g_{xx} is a measure of hydrogen-bonding propensity of the environment of the spin label

The G-tensor

The larger spin-orbit coupling parameter of oxygen relative to nitrogen is the primary source of *g*-anisotropy of the nitroxides. The *G*-tensor anisotropy is related to excitations from the oxygen non-bonding orbitals (*n*-orbitals) into the π^*-orbital (schematically shown in the inset of Fig. 3). Of the three principal directions, the largest effect occurs in the g_x-direction (e.g. Plato et al. 2002). The smaller the excitation energy, the larger the effect on the *g*-tensor. The energy of the *n*-orbitals is lowered by hydrogen bonding to oxygen, and since this increases the energy separation between the *n*- and the π^*-orbitals, g_{xx} decreases with increasing strengths of the hydrogen bonds (Owenius et al. 2001; Plato et al. 2002).

Obviously, similar effects play a role in the more extended π-electron systems of photosynthetic cofactors. Detailed investigations of the distribution of spin density (Allen et al. 2009) and **G-**tensor of these cofactors reveal subtle differences in hydrogen bonding and conformations. The response of the extended π-electron systems of these cofactors to the protein environment seems to be one of the mechanisms by which the protein can fine tune the electronic properties of the cofactors to function optimally.

The light reactions and transient interactions of radicals

Knowledge of the electronic structure and the magnetic resonance parameters of the cofactors in photosynthesis provides the basis for the understanding of the coupling between states and ultimately the electron-transfer properties of the cofactors. These are at the heart of the high efficiency of light-induced charge separation and therefore are much sought after. Intricate experiments such as optically detected magnetic resonance (Carbonera 2009) and the spectroscopy on spin-coupled radical pairs (van der Est 2009) were designed to shed light on these questions. Intriguing is the CIDNP effect measured by solid-state (ss) NMR experiments (Matysik et al. 2009). First of all, the amazing enhancement of the NMR signal intensity by the nuclear spin polarization has attracted attention far beyond the photosynthesis community. After all, the 10,000-fold signal enhancements of CIDNP are a tremendous increase in sensitivity. Apparently, the kinetics of the charge separation and recombination events are such that the nuclear spins become polarized. This polarization is carried over into the diamagnetic ground state of the cofactors and gives rise to the large enhancement of the NMR signals of the diamagnetic states of the cofactors detected by conventional magic-angle spinning NMR. The chemical shift parameters of the nuclei are those of the diamagnetic ground states of these cofactors, whereas the strength of the polarization and therefore the intensity of the signals depend on the hyperfine interactions and the lifetimes of the paramagnetic intermediates of the reaction. Hence, photo-CIDNP MAS NMR allows the study of the photochemical machinery of photosynthetic RCs at atomic resolution in the dark ground state (chemical shifts) as well as in the radical pair state (intensities).

Summary

The symbiosis of magnetic resonance and photosynthesis is a long-standing one, providing insight and challenge for developments in several areas of research. The attraction is long lasting, and the contributions in the remainder of this special issue show that it is a fascinating, multifaceted area of research. The fascination does not end, and maybe, for some it is only beginning.

Acknowledgments It is impossible to do justice to the contributions of the scientists in photosynthesis who contributed to and whose works are cited in this special issue. Personally, I would like to thank my teachers in the field, George Feher, Friedhelm Lendzian, Wolfgang Lubitz, and Klaus Möbius. Maryam Hashemi Shabestari is acknowledged for preparing the figures.

References

Alia A, Ganapathy S, de Groot HJM (2009) Magic Angle Spinning (MAS) NMR to study the spatial and electronic structure of photosynthetic light harvesting complex 2. Photosynth Res (this issue)

Allen JP, Cordova JM, Jolley CC, Murray TA, Schneider JW, Woodbury NW, Williams JC, Niklas J, Klihm G, Reus M, Lubitz W (2009) EPR, ENDOR, and Special TRIPLE measurements of P•+ in wild type and modified reaction centers from Rb. sphaeroides. Photosynth Res 99:1–10

Atherton NM (1993) Principles of electron spin resonance. Ellis Horwood and PTR Prentice Hall, Chichester

Carbonera D (2009) Optically detected magnetic resonance (ODMR) of photoexcited triplet states. Photosynth Res (this issue)

Carrington A, McLachlan AD (1979) Introduction to magnetic resonance. Chapman and Hall, London

Duer MJ (2002) Introduction to solid-state NMR spectroscopy. Wiley-Blackwell Publishing, Oxford

Feher G (1998) Three decades of research in bacterial photosynthesis and the road leading to it: a personal account. Photosynth Res 55:3–40

Finiguerra MG, Blok H, Ubbink M, Huber M (2006) High-field (275 GHz) spin-label EPR for high-resolution polarity determination in proteins. J Magn Reson 180:197–202

Flores M, Isaacson R, Abresch E, Calvo R, Lubitz W, Feher G (2007) Protein-cofactor interactions in bacterial reaction centers from Rhodobacter sphaeroides R-26: II. Geometry of the hydrogen bonds to the primary quinone Q(A)(-) by H-1 and H-2 ENDOR spectroscopy. Biophys J 92:671–682

Hore PJ (1995) Nuclear magnetic resonance. Oxford University Press, Oxford

Kothe G, Thurnauer MC (2009) What you get out of high-time resolution electron paramagnetic resonance—example from photosynthetic bacteria. Photosynth Res (this issue)

Kulik L, Lubitz W (2009) Electron–nuclear double resonance. Photosynth Res (this issue)

Levitt MH (2008) Spin dynamics. Basics of nuclear magnetic resonance. Wiley, Chichester

Matysik J, Diller A, Roy E, Alia A (2009) The solid-state photo-CIDNP effect. Photosynth Res (this issue)

Owenius R, Engström M, Lindgren M, Huber M (2001) Influence of solvent polarity and hydrogen bonding on the EPR parameters of a nitroxide spin label studied by 9-GHz and 95-GHz EPR spectroscopy and DFT calculations. J Phys Chem A 105:10967–10977

Plato M, Steinhoff HJ, Wegener C, Törring JT, Savitsky A, Möbius K (2002) Molecular orbital study of polarity and hydrogen bonding effects on the g and hyperfine tensors of site directed NO spin labelled bacteriorhodopsin. Mol Phys 100:3711–3721

Savitzky A, Möbius K (2009) High-field EPR. Photosynth Res (this issue)

Schweiger A, Jeschke G (2001) Principles of pulse electron paramagnetic resonance. Oxford University Press, Oxford

Slichter CP (1996) Principles of magnetic resonance. Springer, Berlin

van der Est A (2009) Transient EPR: using spin polarization in sequential radical pairs to study electron transfer in photosynthesis. Photosynth Res (this issue)

van Gastel M (2009) Pulsed EPR spectroscopy. Photosynth Res (this issue)

Weil JA, Bolton JR (2007) Electron paramagnetic resonance: elementary theory and practical applications. Wiley, Chichester